International Journal of Thermophysics, Vol. 20, No. 1, 1999

Vapor–Liquid Equilibria of Alternative Refrigerants by Molecular Dynamics Simulations[1]

M. Lísal,[2] R. Budinský,[3] V. Vacek,[3] and K. Aim[2,4]

Alternative refrigerants HFC-152a (CHF_2CH_3), HFC-143a (CF_3CH_3), HFC-134a (CF_3CH_2F), and HCFC-142b (CF_2ClCH_3) are modeled as a dipolar two-center Lennard–Jones fluid. Potential parameters of the model are fitted to the critical temperature and vapor–liquid equilibrium data. The required vapor–liquid equilibrium data of the model fluid are computed by the Gibbs–Duhem integration for molecular elongations $L = 0.505$ and 0.67, and dipole moments $\mu^{*2} = 0$, 2, 4, 5, 6, 7, and 8. Critical properties of the model fluid are estimated from the law of rectilinear diameter and critical scaling relation. The vapor–liquid equilibrium data are represented by Wagner equations. Comparison of the vapor–liquid equilibrium data based on the dipolar two-center Lennard–Jones fluid with data from the REFPROP database shows good-to-excellent agreement for coexisting densities and vapor pressure.

KEY WORDS: alternative refrigerants; Gibbs–Duhem integration; HCFC-142b; HFC152a; HFC-143a; HFC-134a; Lennard–Jones two-center dipolar potential model; molecular simulations; vapor–liquid equilibria.

1. INTRODUCTION

In several recent papers it has been demonstrated that good-to-excellent prediction of the thermodynamic and vapor-liquid equilibrium (VLE) data of pure fluids can be obtained by molecular simulations [1]. A crucial point in this computer modeling of real substances is the determination of effective molecular interaction potentials. For the ethane-type alternative

[1] Paper presented at the Thirteenth Symposium on Thermophysical Properties, June 22–27, 1997, Boulder, Colorado, U.S.A.

[2] E. Hála Laboratory of Thermodynamics, Institute of Chemical Process Fundamentals, Academy of Sciences, 165 02 Prague 6, Czech Republic.

[3] Department of Physics, Czech Technical University, 167 06 Prague 6, Czech Republic.

[4] To whom correspondence should be addressed.

0195-928X/99/0100-0163$16.00/0

refrigerants, an atom–atom potential predicts very well both the thermodynamic and the structural properties [2].

If we primarily focus on the thermodynamic and VLE data, simple two-center Lennard–Jones potential with a point dipole (2CLJD) gives results with an accuracy equivalent to the atom–atom potential [3, 4], but with much less demand on computer time. The 2CLJD potential approximates reasonably well the "diatomic" character of the ethane-type alternative refrigerants as well as van der Waals and electrostatic interactions. The 2CLJD potential has four parameters: molecular elongation L, energy and size parameters ε and σ, and dipole moment μ^* that must be fitted to selected experimental data [1, 3–5].

The aim of the present paper is to study the ethane-type alternative refrigerants HFC-152a (CHF_2CH_3), HFC-143a (CF_3CH_3), HFC-134a (CF_3CH_2F), and HCFC-142b (CF_2ClCH_3). For this purpose, we computed VLE of the 2CLJD fluids for molecular elongations $L = 0.505$ and 0.67, and dipole moments $\mu^{*2} = 0, 2, 4, 5, 6, 7$, and 8. Subsequently, we fitted the potential parameters of the ethane-type alternative refrigerants to the obtained VLE data. Further, we compared VLE data based on the 2CLJD fluid with data from the REFPROP database [6].

2. POTENTIAL MODEL

The 2CLJD model of the ethane-type alternative refrigerants consists of two interaction centers at a distance l apart and a point dipole $\boldsymbol{\mu}$ in the center of the molecule. The interaction centers interact via the Lennard–Jones 12–6 potential. The intermolecular potential for the 2CLJD fluid, u_{2CLJD}, is

$$u_{2CLJD}(r, \omega_i, \omega_j) = u_{2CLJ}(r, \omega_i, \omega_j) + u_D(r, \omega_i, \omega_j) \tag{1}$$

where r is the distance between centers of mass of molecule j and molecule i, and ω_i, ω_j is the orientation of molecules. The 2CLJ interaction, u_{2CLJ}, is defined as

$$u_{2CLJ}(r, \omega_i, \omega_j) = \sum_{a=1}^{2} \sum_{b=1}^{2} 4\varepsilon \left[\left(\frac{\sigma}{r_{ab}} \right)^{12} - \left(\frac{\sigma}{r_{ab}} \right)^{6} \right] \tag{2}$$

In Eq. (2), r_{ab} is the distance between atom a of molecule i and atom b of molecule j, and ε and σ are the Lennard–Jones energy and size parameters, respectively. The interaction between two point dipoles $\boldsymbol{\mu}_i$ and $\boldsymbol{\mu}_j$, u_D, is given as

$$u_D(r, \omega_i, \omega_j) = -\boldsymbol{\mu}_i \mathbf{T}(\mathbf{r}) \boldsymbol{\mu}_j \tag{3}$$

where $\mathbf{r} = \mathbf{r}_j - \mathbf{r}_i$ is the distance vector between centers of mass of molecules j and i. The dipole–dipole tensor $\mathbf{T}(\mathbf{r})$ is

$$T_{ab} = \frac{3r_a r_b}{r^5} - \frac{\delta_{ab}}{r^3} \tag{4}$$

with Kronecker's symbol δ_{ab}.

The approximation of fluorinated ethanes as homonuclear two-center molecules is not too severe because the fluorine atom is relatively small. The same approximation for HCFC-142b is doubtful due to size of the chlorine atom; HCFC-142b resembles more the shape of propane. However, calculation of the second virial coefficient for HCFC-142b on the basis of the 2CLJD model potential showed a good agreement with experimental data [3]. The dipole vector does not lie along the molecular axis in HFC-152a, HFC-134a and HCFC-142b molecules. According to the finding of Vega et al. [4] (namely, that for a dipole vector forming some angle with the molecular axis, a smaller value of the dipole moment is required to produce similar thermodynamic properties as for the case when the dipole vector lies along the molecular axis) and with the intention to reduce number of potential parameters, we have assumed that the dipole vector lies along the molecular axis.

For model fluids, we used the Lennard–Jones reduced units: $L = l/\sigma$, $r^* = r/\sigma$, $t^* = t/(\sigma\sqrt{(m/\varepsilon)})$, $T^* = k_B T/\varepsilon$, $\rho^* = \rho\sigma^3$, $p^* = p\sigma^3/\varepsilon$, $u^* = u/N\varepsilon$, $h^* = h/N\varepsilon$, $B^* = B/\sigma^3$, and $\mu^{*2} = \mu^2/(4\pi\varepsilon_0\varepsilon\sigma^3)$.

3. VLE FOR 2CLJD FLUIDS

Vega et al. [4] used the molecular elongation $L = 0.505$ for the 2CLJD model of HFC-152a. For the 2CLJ model of ethane, $L = 0.67$ was found [8]. The second virial coefficients of the investigated refrigerants based on the 2CLJD model potential gave $L \approx 0.7$ [3]. Hence, we generated VLE data needed to fit the potential parameters for $L = 0.505$ and 0.67 (to be consistented with previously studied molecular elongations [9]), and $\mu^{*2} = 0$, 2, 4, 5, 6, 7, and 8 (to cover expected values of effective dipole moments [4]). The required VLE data were computed by the Gibbs–Duhem integration [10]. The Gibbs–Duhem integration solves numerically the Clapeyron equation,

$$\left(\frac{d \ln p^*}{d(1/T^*)}\right)_\sigma = -\frac{T^*}{p^*} \frac{h_v^* - h_l^*}{1/\rho_v^* - 1/\rho_l^*} \tag{5}$$

and evaluates the right-hand side of the Clapeyron equation from molecular simulations. In Eq. (5), h_v^*, and h_l^*, are the vapor and liquid enthalpies, and ρ_v^* and ρ_l^* are the vapor and liquid number densities; the subscript σ indicates that the derivative is taken along the saturation line. We evaluated the right-hand side of the Clapeyron equation by means of constant pressure–constant temperature (NPT) molecular dynamics (MD) simulations. Further details about the application of the Gibbs–Duhem integration to the 2CLJD fluids can be found in Ref. [11].

VLE data of the 2CLJD fluids were represented by Wagner equations [12]. First, we estimated the critical temperature T_C^* and density ρ_C^* from a least-squares fit of the law of rectilinear diameter [10],

$$\frac{\rho_l^* + \rho_v^*}{2} = \rho_C^* \quad C_1(T^* - T_C^*) \tag{6}$$

and critical scaling relation [10],

$$\rho_l^* - \rho_v^* = C_2(T_C^* - T^*)^{0.325} \tag{7}$$

The fit of Eq. (6) was performed over the whole temperature range and that of Eq. (7) for temperatures in the proximity of expected critical point. Critical temperatures T_C^* and densities ρ_C^* as well as coefficients C_1 and C_2 are listed in Table I.

Table I. Critical Temperatures T_C^* and Densities ρ_C^*, and Coefficients C_1 and C_2 of Eqs. (6) and (7) for the Dipolar Two-Center Lennard–Jones Fluids

L	μ^{*2}	T_C^*	ρ_C^*	C_1	C_2
0.505	0	2.7127	0.2000	−0.06129	0.5140
	2	2.7498	0.2062	−0.05643	0.5240
	4	2.9102	0.2035	−0.05609	0.5175
	5	3.0331	0.2008	−0.05608	0.4803
	6	3.1534	0.1959	−0.05780	0.4835
	7	3.2314	0.1946	−0.05738	0.4838
	8	3.2669	0.2014	−0.05304	0.4993
0.67	0	2.2598	0.1738	−0.06785	0.4871
	2	2.3277	0.1744	−0.06550	0.4745
	4	2.4375	0.1770	−0.06117	0.4744
	5	2.5038	0.1674	−0.07067	0.4752
	6	2.5864	0.1706	−0.06459	0.4682
	7	2.6666	0.1698	−0.06339	0.4679
	8	2.7691	0.1683	−0.06162	0.4530

Table II. Critical Pressures p_C^* and Coefficients N_{1p} to N_{4p} of the Wagner Vapor–Pressure Eq. (8) for the Dipolar Two-Center Lennard–Jones Fluids

L	μ^{*2}	p_C^*	N_{1p}	N_{2p}	N_{3p}	N_{4p}
0.505	0	0.15243	−5.76229	0.19129	1.07695	−14.14945
	2	0.16828	−7.49298	3.99085	−3.60826	−1.55688
	4	0.17221	−6.63795	1.76673	−1.77045	−0.91049
	5	0.19048	−6.47781	1.28378	−1.16767	−4.59751
	6	0.18017	−5.87938	0.32693	−1.01893	−3.70698
	7	0.18175	−6.00254	0.26149	−1.15386	−4.15584
	8	0.18709	−6.23273	−0.31780	−0.30368	−3.86139
0.67	0	0.10919	−6.05222	0.63426	−0.11831	−4.58783
	2	0.12044	−6.44046	1.83295	−2.96131	5.73485
	4	0.12908	−6.94920	2.43143	−3.43178	4.18114
	5	0.10714	−4.64389	−3.25747	3.57765	−13.62441
	6	0.11891	−5.89604	−0.15821	−1.39170	2.78797
	7	0.11962	−6.08119	−0.00662	−1.59808	−2.49514
	8	0.12349	−5.95864	0.11212	−3.41970	7.36303

Then vapor pressures p_σ^* were fitted to Wagner equation [12],

$$\ln\left(\frac{p_\sigma^*}{p_C^*}\right)=\left(\frac{T_C^*}{T^*}\right)(N_{1p}\tau+N_{2p}\tau^{3/2}+N_{3p}\tau^{5/2}+N_{4p}\tau^5) \tag{8}$$

where $\tau=1-T^*/T_C^*$. Critical pressures p_C^* and coefficients N_{1p} to N_{4p} are listed in Table II.

Finally, to correlate coexistence envelopes analytically, we utilized Wagner expressions [12] for description of saturated-liquid densities ρ_l^*,

$$\ln\left(\frac{\rho_l^*}{\rho_C^*}\right)=N_{1l}\tau^{2/6}+N_{2l}\tau^{3/6}+N_{3l}\tau^{7/6}+N_{4l}\tau^{9/6} \tag{9}$$

and saturated-vapor densities ρ_v^*,

$$\ln\left(\frac{\rho_v^*}{\rho_C^*}\right)=N_{1v}\tau^{2/6}+N_{2v}\tau^{4/6}+N_{3v}\tau^{7/6}+N_{4v}\tau^{13/6}+N_{5v}\tau^{25/6} \tag{10}$$

Coefficients N_{1l} to N_{4l}, and N_{1v} to N_{5v} are listed in Table III.

4. POTENTIAL PARAMETERS

The 2CLJD model has four adjustable potential parameters $L=l/\sigma$, ε, σ and $\mu^*=\mu/\sqrt{4\pi\varepsilon_0\varepsilon\sigma^3}$ that must be fitted to selected experimental

Table III. Coefficients N_{1l} to N_{4l} and N_{1v} to N_{5v} of the Wagner Eqs. (9) and (10) for the Dipolar Two-Center Lennard–Jones Fluids

L	μ^{*2}	N_{1l}	N_{2l}	N_{3l}	N_{4l}	N_{1v}	N_{2v}	N_{3v}	N_{4v}	N_{5v}
0.505	0	1.88053	−0.66318	−0.27473	0.41603	−1.86845	−1.38974	−2.85533	−7.4643	−22.92178
	2	2.12780	−1.07399	−0.17297	0.50663	0.71368	−9.48000	4.71870	−6.8159	−28.35696
	4	1.98716	−0.79488	−0.41739	0.59935	−1.58047	−2.27635	−2.83483	−6.7548	−11.00512
	5	1.09861	0.63795	−1.43340	1.02487	0.00454	−10.39990	18.85571	−51.3156	1.73681
	6	2.18187	−1.32892	1.52854	−14056	0.05140	−10.47372	14.72511	−31.2193	2.63390
	7	2.21032	−1.33094	1.50335	−1.14624	0.05243	−10.55007	14.82780	−32.0958	2.42544
	8	1.86454	−0.61074	−0.15324	0.20241	−0.95000	−3.90816	−1.78326	−7.1649	−22.13303
0.67	0	1.93009	−0.68266	−0.39790	0.55384	−1.13411	−4.80648	1.45775	−3.2040	−82.61405
	2	1.70765	−0.35149	−0.57216	0.59581	−0.52042	−5.85345	1.43874	−2.9501	−65.82161
	4	1.80901	−0.50009	−0.66937	0.76756	−1.25514	−3.49632	−0.33486	−12.0474	−4.02530
	5	2.15300	−1.12387	1.27791	−1.08947	0.00919	−13.07564	21.61751	−40.2735	2.82401
	6	2.22535	−1.29740	1.42924	−1.14537	0.02517	−11.32230	16.08758	−33.0521	2.05221
	7	2.24899	−1.28276	1.17479	−0.88436	0.05863	−12.28265	18.81286	−37.2884	0.53174
	8	1.64697	−0.20823	−0.29194	0.19330	−1.17936	−4.74726	0.63328	−2.6697	−75.78410

data. However, the dipole moment p and molecular elongation l should be varied between small limits for consistency with (i) an experimental value of the dipole moment and molecular polarizability (see Table IV, where some general properties are listed) and (ii) a size of the molecule. It is recognized that an enhanced (effective) dipole moment takes into account reasonably well an induced dipole caused by the molecular polarizability [2] and effects of the angle that form the dipole vector with the molecular axis in HFC-152a, HFC-143a, HFC-134a, and HCFC-142b molecules [4].

In the most often used method, potential parameters are derived from experimental low-density properties (the second virial coefficient or gaseous viscosity; see references in Ref. [5]) Disadvantages of this method are that (i) neither the potential parameters derived from the second virial coefficient nor those derived from the gaseous viscosity, and/nor those derived simultaneously from the second virial coefficient and gaseous viscosity give consistent values, and (ii) the potential parameters lead to a good description of low-density properties but fail to reproduce properties in the liquid-like region.

In the liquid-like region, many-body interactions play a significant role. The potential parameters derived from the low-density properties, and thus based on only two-body interactions, cannot work properly in this region. However, if appropriate experimental properties from the liquid-like region are involved in the adjustment of the potential parameters, the potential parameters effectively contain many-body effects. Studies on the departure from the principle of corresponding states show that the critical temperature, the slope of the vapor pressure curve, the saturated-liquid densities, and heat of vaporization depend most strongly on the dipole moment and molecular elongation [13]. If we assume the same behavior of the departure from the principle of corresponding states for real and underlying model fluids, the essential idea of our adjustment is (i) to fit ε to the experimental critical temperature and σ to the experimental saturated-liquid density at one temperature (we chose $T=0.75T_C$ [5]) and (ii) to adjust the dipole moment to the steepness of the vapor pressure curve.

Table IV. General Properties of the Investigated Alternative Refrigerants [6]

Refrigerant	$M \times 10^3$ ($kg \cdot mol^{-1}$)	μ (D)	α ($Å^3$)	T_C (K)	ρ_C ($kg \cdot m^{-3}$)	p_C (kPa)
HFC-152a	66.05	2.262	4.26	386.7	368	4492
HFC-143a	84.04	2.34	4.40	346.25	455	3834.3
HFC-134a	102.03	2.058	4.58	374.3	515	4060.3
HCFC-142b	118.49	2.14	6.42	410.3	435	4120

Table V. Potential Parameters of the Investigated Alternative Refrigerants Derived from the VLE Data (In Parentheses, the Potential Parameters Derived from the Second Virial Coefficient [3])

Refrigerant	l (Å)	σ (Å)	ε/k_B (K)	μ (D)
HFC-152a	2.464	3.678	145.0	2.641
	(2.546)	(3.690)	(154.0)	(2.26, 70°[a])
HFC-143a	2.541	3.793	129.8	2.617
	(2.621)	(3.745)	(155.0)	(2.36, 0°[a])
HFC-134a	2.559	3.819	140.4	2.749
	(2.677)	(3.770)	(167.7)	(2.07, 85°[a])
HCFC-142b	2.677	3.996	153.9	3.080
	(2.847)	(3.900)	(200.0)	(2.16, 30°[a])

[a] The 2CLJD model of Kohler and Van Nhu [3] takes into account the angle between the dipole vector and the molecular axis.

We performed the adjustment for both elongations $L = 0.505$ and 0.67 and allowed dipole moments to be higher than experimental values (to take into account effects of the molecular polarizability and angle between the dipole vector and molecular axis). we found that the 2CLJD model with $L = 0.67$ and $\mu^{*2} = 7$ represents best the steepness of the vapor–pressure curve for all investigated refrigerants. The derived potential parameters based on this model are listed in Table V. In Table V, we also included the potential parameters derived from the second virial coefficients [3]. From Table V, we can see that (i) l's and σ's are similar in both potential parameters sets, (ii) ε's derived from the second virial coefficient are higher than those derived from the VLE data, and (iii) μ's derived from the VLE data are $\approx 20\%$ higher (except HCFC-142b) than experimental (gaseous) dipole moments.

5. RESULTS

We present a comparison between VLE data calculated from the 2CLJD fluid and REFPROP database [6] in Figs. 1 to 4 for the coexisting densities and vapor pressure. Reported uncertainties of the REFPROP saturated-liquid densities are up to 3%. One can see from Figs. 1 to 4 that the agreement between the calculated and the REFPROP saturated liquid densities is excellent for all investigated alternative refrigerants. The calculated saturated-liquid densities lie within the estimated experimental

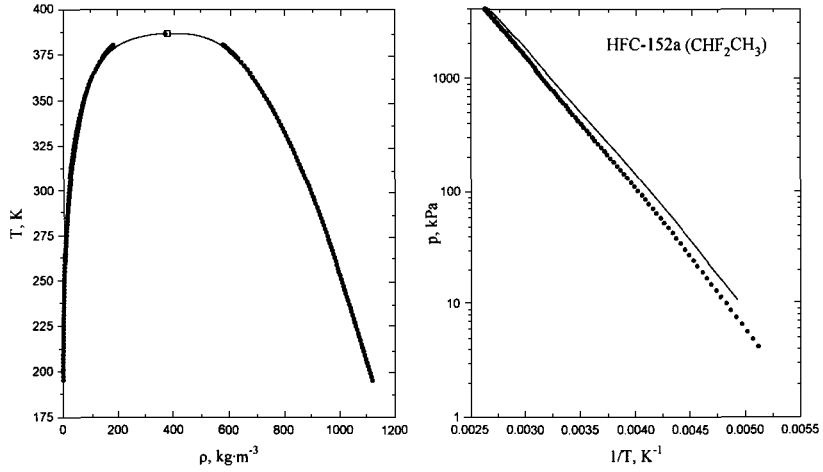

Fig. 1. Phase-coexistence and vapor–pressure curves for HFC-152a (CHF_2CH_3). (•): Data from the REFPROP database [6]; (—) this work. The critical point on the phase coexistence curve is indicated by the square.

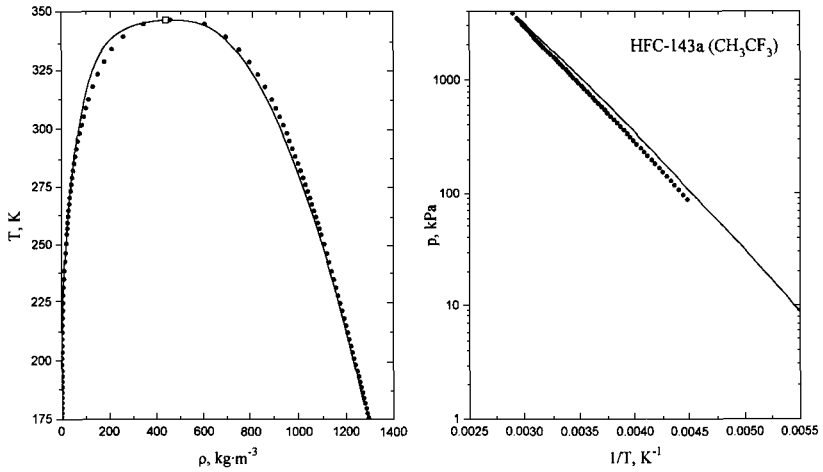

Fig. 2. Phase-coexistence and vapor–pressure curves for HFC-143a (CF_3CH_3). (•): Data from the REFPROP database [6]; (—) this work. The critical point on the phase coexistence curve is indicated by the square.

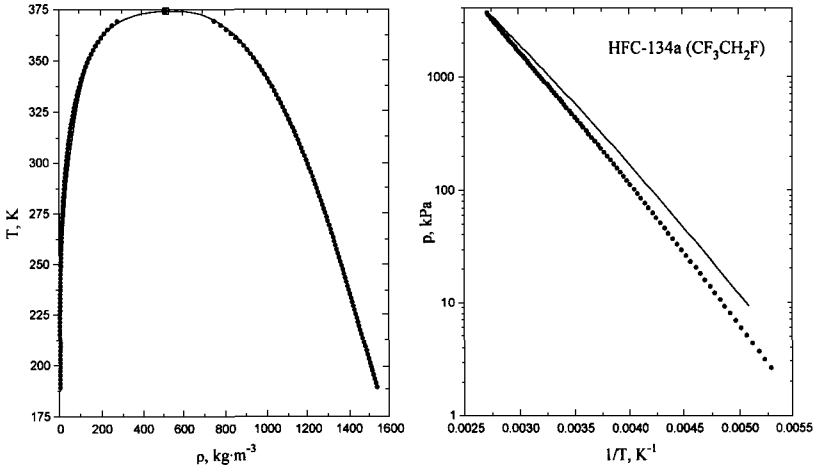

Fig. 3. Phase-coexistence and vapor–pressure curves for HFC-134a (CF_3CH_2F). (•): Data from the REFPROP database [6]; (—) this work. The critical point on the phase coexistence curve is indicated by the square.

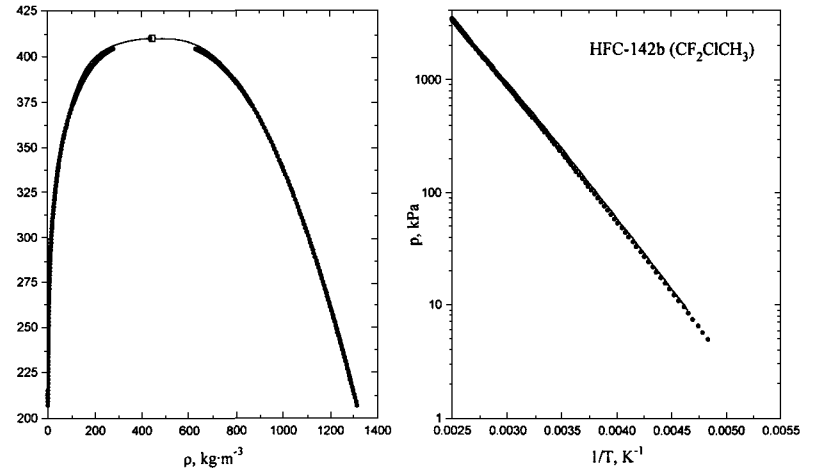

Fig. 4. Phase-coexistence and vapor–pressure curves for HCFC-142b (CF_2ClCH_3). (•): Data from the REFPROP database [6]; (—) this work. The critical point on the phase coexistence curve is indicated by the square.

uncertainty. As seen from Figs. 1 to 4, the agreement between the calculated and the REFPROP vapor pressures is good for the investigated alternative refrigerants. The calculated vapor pressures are systematically higher than REFPROP values.

6. CONCLUSIONS

We modeled alternative refrigerants HFC-152a (CHF_2CH_3), HFC-143a (CF_3CH_3), HFC-134a (CF_3CH_2F), and HCFC-142b (CF_2ClCH_3) as the 2CLJD fluid. The 2CLJD potential parameters for a particular alternative refrigerant were derived by forcing the critical temperature, one saturated-liquid density and the steepness of the vapor-pressure curve of a 2CLJD fluid to correspond to that of the alternative refrigerant. VLE data of underlying 2CLJD model fluids were computed by the Gibbs–Duhem integration method. We found that the 2CLJD model fluid with $L = 0.67$ and $\mu^{*2} = 7$ best represents phase coexistence data of all investigated alternative refrigerants. Agreement between VLE data (saturated densities and vapor pressure) calculated from the 2CLJD fluid and those from the REFPROP database was good to excellent for the investigated alternative refrigerants.

ACKNOWLEDGMENTS

The authors would like to acknowledge the support of the Grant Agency of the Academy of Sciences of the Czech Republic (Grant No. A-4072712), the Grant Agency of the Czech Republic (Grant No. 1397004), and FR VŠ (Grant No. 1084/97). Calculations were made on the IBM SP2 in the Joint Computer Centre of Czech Technical University, Institute of Chemical Technology, and IBM Czech Republic, Prague.

REFERENCES

1. C. Kriebel, A. Muller, J. Winkelmann, and J. Fischer, *Int. J. Thermophys.* **17**:1349 (1996), and Refs. 1–12 therein.
2. M. Lísal and V. Vacek, *Mol. Phys.* **87**:167 (1996); *Fluid Phase Equil.* **127**:83 (1997).
3. F. Kohler and N. Van Nhu, *Mol. Phys.* **80**:795 (1993).
4. C. Vega, B. Saager, and J. Fischer, *Mol. Phys.* **68**:1079 (1989).
5. M. E. van Leeuwen, *Fluid Phase Equil.* **99**:1 (1994).
6. J. Gallagher, M. McLinden, G. Morrison, and M. Huber, *NIST Thermodynamic Properties of Refrigerants and Refrigerant Mixtures Database (REFPROP), NIST Std. Ref. Database 23, Version 5.0* (NIST, Boulder, CO, 1993).
7. M. P. Allen and D. J. Tildesley, *Computer Simulation of Liquids* (Clarendon Press, Oxford, 1987).

8. J. Fischer, R. Lustig, H. Breitenfelder-Manske, and W. Lemming, *Mol. Phys.* **52**:485 (1984).
9. Ch. Kriebel, A. Müller, J. Winkelmann, and J. Fischer, *Mol. Phys.* **84**:381 (1995).
10. D. A. Kofke, *J. Chem. Phys.* **98**:4149 (1993).
11. M. Lísal and V. Vacek, *Mol. Sim.* **17**:27 (1996); M. Lísal, R. Budinský, and V. Vacek, *Fluid Phase Equil.* **135**:193 (1997).
12. W. Duschek, R. Kleinrahm, and W. Wagner, *J. Chem. Thermodyn.* **22**:841 (1990).
13. B. Garzón, S. Lago, C. Vega, and L. F. Rull, *J. Chem. Phys.* **102**:7204 (1995); C. Vega, S. Lago, and B. Garzón, *J. Chem. Phys.* **98**:11181 (1994).